Characterization of Fixture-Workpiece Static Friction

By

Jose F. Hurtado
Shreyes N. Melkote

Precision Manufacturing Research Consortium
Georgia Institute of Technology

Sponsors: NSF, GM R&D Center

Background

- Critical Functions of a Machining Fixture:
  - Accurately locate and hold a workpiece with respect to the cutting tool.
  - Minimize workpiece movement and distortion due to clamping and machining.
- Fixture performance depends on contact forces and friction, e.g. mechanical vise.

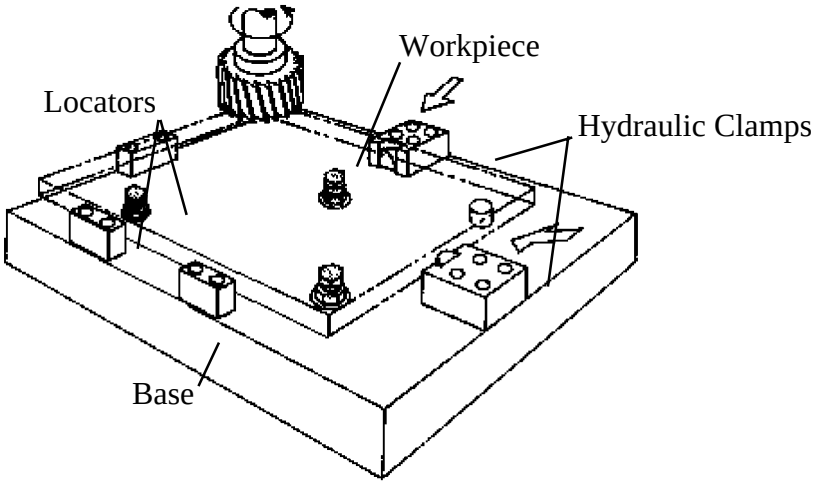

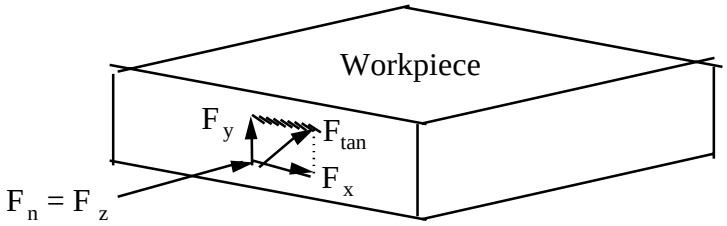

$$F_{\tan} < \mu_s F_n$$

F_{tan} = tangential force
F_n = normal force
μ_s = static coefficient of friction

Motivation

- Scientific understanding of the effects of workpiece, fixture and cutting process variables on workpiece-fixture contact forces and friction is limited.
- Factors of interest are those affecting the workpiece-fixture interface such as contact geometry, workpiece stiffness, surface finish and machining conditions.
- The understanding of these variables on workpiece-fixture contact force and friction, especially, under dynamic conditions is needed.

Objectives

- Experimentally study the effects of vibration and clamping load on the static coefficient of friction, μ_s.

- Prediction of workpiece-fixture contact forces during machining based on an empirical model for dynamic friction.

Study of Dynamic Friction

- **Objective:** Understand the effect of oscillatory forces and vibration on the static coefficient of friction for a workpiece-fixture material pair.
- **Materials Considered:**
  - Cast Aluminum 357 (Workpiece)
  - Steel AISI 1144 with Black Oxide Finish (Locator)
- **Working Principle of the Test Stand:**

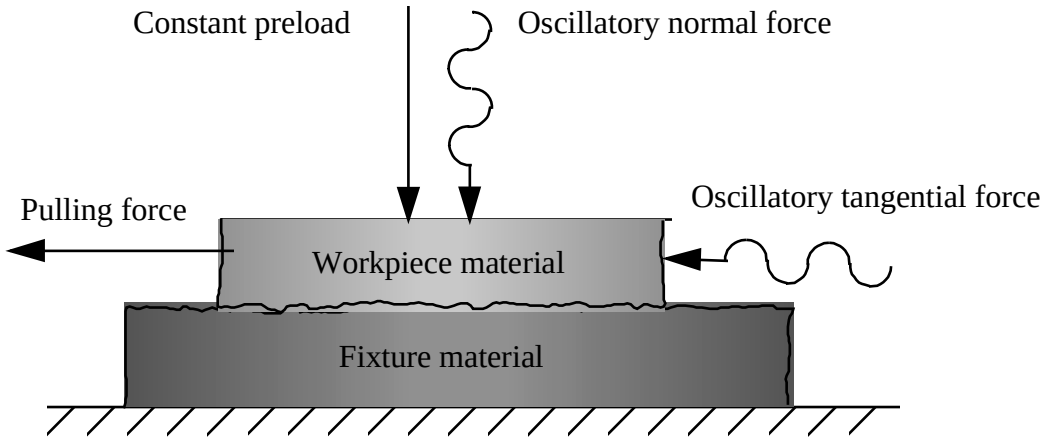

Experimental Set-Up

1. Linear stepper motor. Servo Systems 23A-6102A.
2. Strain gauge. Omegadyne LC-105.
3. Base plate.
4. Link.
5. Displacement probe. Kaman KD1106-1S, KD2300-2S.
6. Accelerometer. PCB Electronics 356A11.
7, 11, 18. Triaxial load cell. Kistler 9117A.
8. Preloading bolt. Kistler 9461.
9. Locator material holder.
10. Workpiece material sample.
12, 17. Piezoelectric pusher. Burleigh PZL-060.
13. Angle bracket. Carr Lane CL-13-GAB.
14. Thrust bearing. 1 in. O.D.
15. Stainless steel sliding plate.
16. Support.

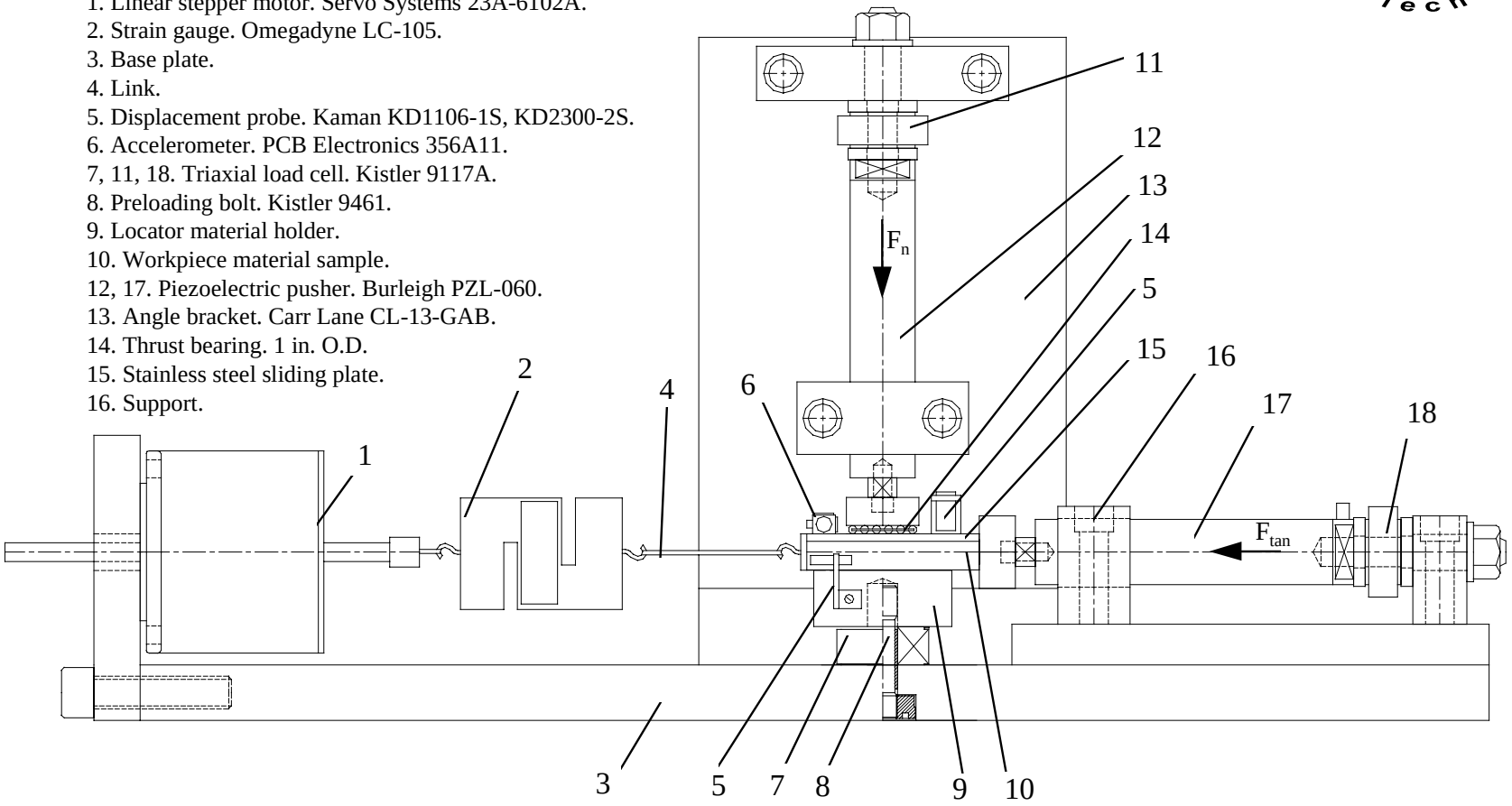

Experimental Design

- **Experimental Design:** Central Composite Design. 2 x 27 Test Runs.
- **Factor A:** Normal Preload Force.

  Low: 100 N Medium: 200 N High: 300 N
- **Factor B:** Vibration Amplitude in the Normal Direction.

  Low: 0 μm Medium: 2.5 μm High: 5.0 μm
- **Factor C:** Excitation Frequency in the Normal and Tangential Directions.

  Low: 100 Hz Medium: 150 Hz High: 200 Hz
- **Factor D:** Vibration Amplitude in the Tangential Direction.

  (Not controlled at fixed levels)
- **Response:**

$$\mu_s = \frac{\overline{F}_{\tan}}{\overline{F}_n} \longrightarrow \mu_{\text{s,novib}} \quad \mu_{\text{s,extvib}}$$

Results

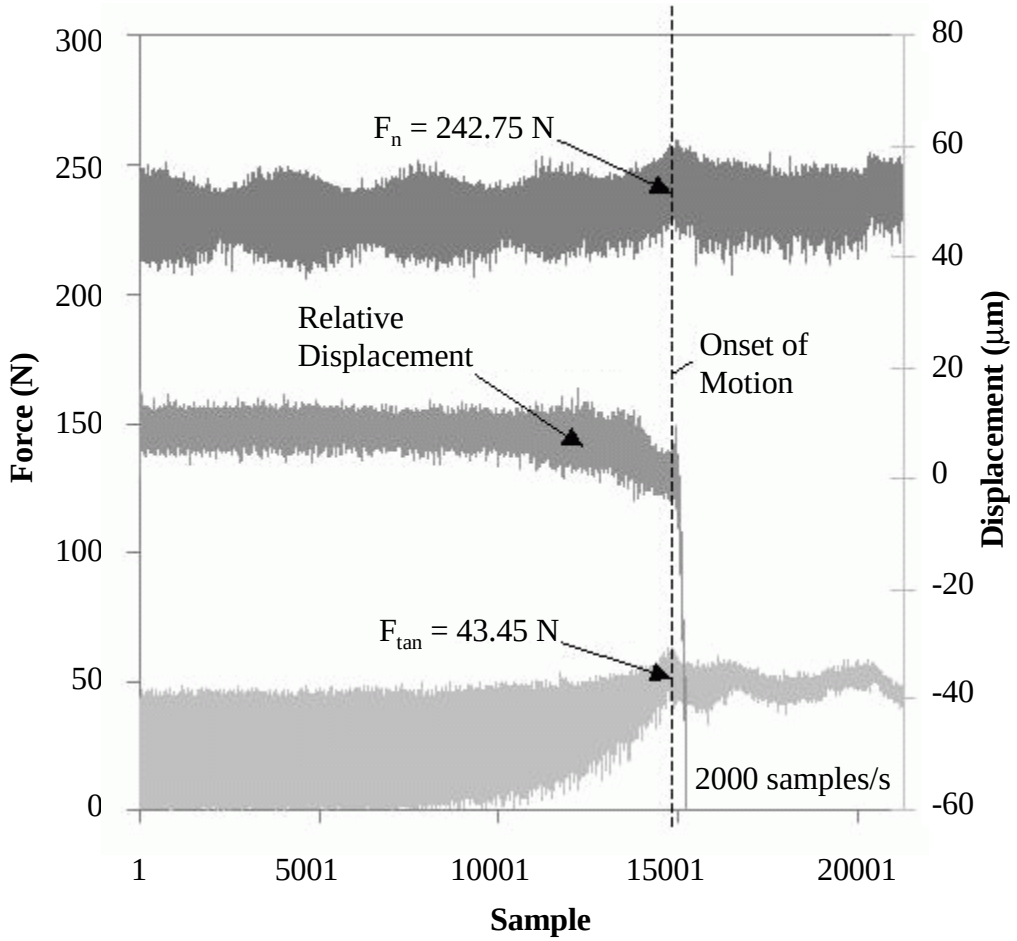

Data from Test #16

Results

- Maximum reduction in μ_s = 61%

$$\% \text{ Change } = \left(\frac{\mu_{s,extvib} - \mu_{s,novib}}{\mu_{s,novib}}\right)100\%$$

- A second-order response surface was fit to the collected data. R^2 = 81.2 %.
- The following effects are significant for α = 5 %:
  - Preload force
  - Normal amplitude
  - Normal/Tangential Frequency
  - Preload Force * Normal Amplitude
  - Preload Force * Frequency
  - Normal Amplitude * Tangential amplitude
  - Frequency * Tangential Amplitude
  - Preload Force * Tangential Amplitude (only for α = 10 %)

Response Surface for $\mu_{s,extvib}$

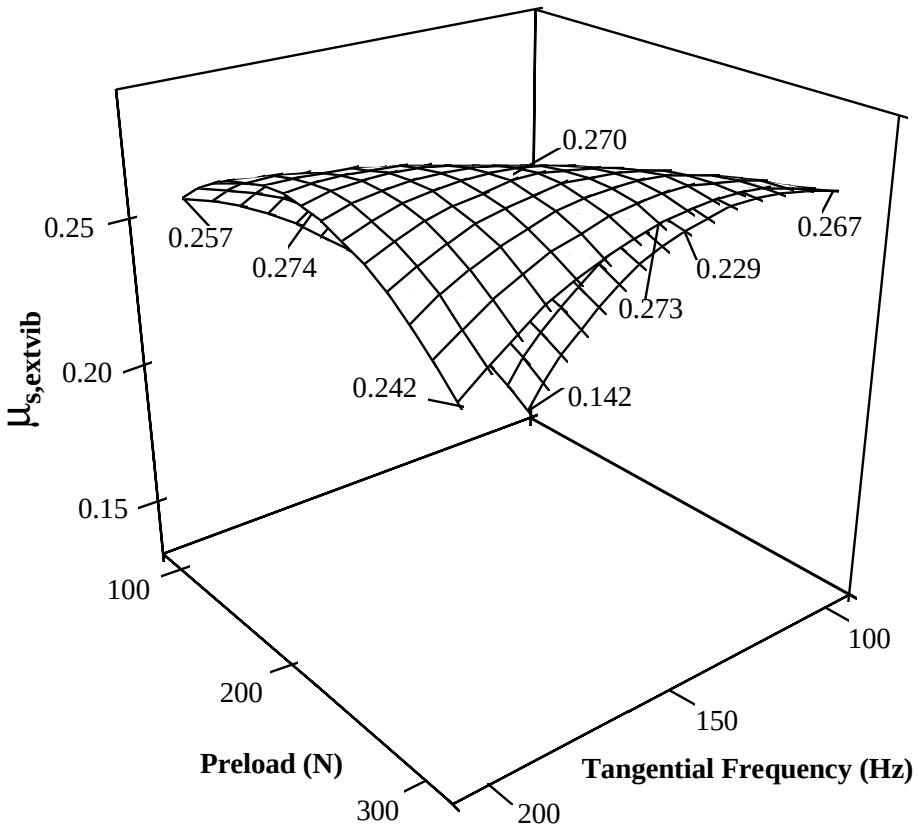

Low-Intensity Machining Process. Normal Amplitude = 0 μm, Tangential Amplitude = 5.2 μm.

Response Surface for $\mu_{s,extvib}$

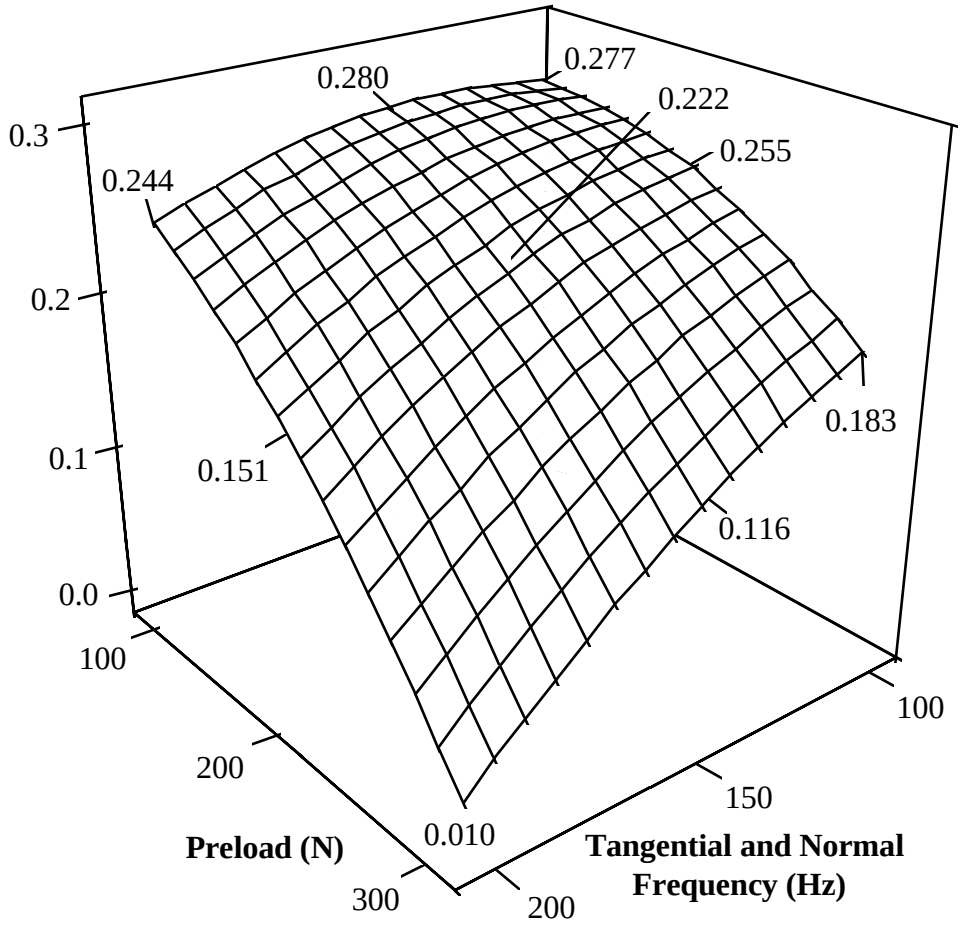

High-Intensity Machining Process. Normal Amplitude = 5 μm, Tangential Amplitude = 22.7 μm.

Explanations

- Increase in $\mu_{s,extvib}$ with increasing excitation frequency at low normal preloads was attributed to breakdown of contaminant layers due to vibration.
- Decrease in $\mu_{s,extvib}$ with increasing frequency at high normal preloads was attributed to decrease in duration of asperity contact and possible resonance.
- The increase in $\mu_{s,extvib}$ with increasing preload was explained by the increase in the actual contact area with increasing normal preload.

Prediction of Reaction Forces

- **Free Body Diagram of the Workpiece.**

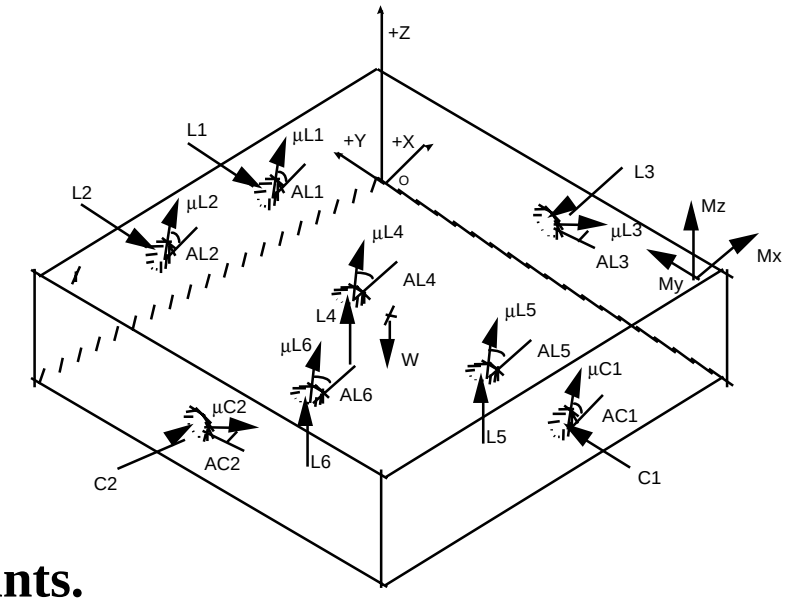

- **System Constraints.**
  - Force equilibrium.
  - Moment equilibrium.
  - Direction of the normal contact force.
  - Maximum normal force.

Prediction of Reaction Forces

- **Summary of Results:**
  - The model is in good agreement with reaction forces at a specific locator when only clamping forces are applied.
  - The accuracy of the model can be improved by using estimated values of μ_s under dynamic conditions similar to those present during machining.

Test Condition	Relative Errors (%)			
	Average		Maximum	
	F_{tan}	F_n	F_{tan}	F_n
Clamping Only	4.2	-3.9	10.6	-6.5
Machining Using $\mu_{s,novib}$	16	-9.8	42.4	-11.2
Machining Using $\mu_{s,extvib}$	-3.4	-5.3	18.4	-8.5

Conclusions

- There is a significant difference between the static coefficient of friction under dynamic and non-dynamic conditions.
- Preload force, amplitude of oscillation in the normal direction and frequency of externally applied loads are significant first-order factors affecting $\mu_{s,extvib.}$
- At low preload forces and for low- and medium-intensity machining processes, increasing the excitation frequency causes an increase in $\mu_{s,extvib.}$
- As the preload force and/or the intensity of the machining process increase, the effect of the excitation frequency is to lower $\mu_{s,extvib.}$

Future Work

- Study the effect of the following factors on the static coefficient of friction under dynamic conditions, $\mu_{s,extvib}$:
  - Cutting fluids
  - Higher normal preloads
  - Phase of the normal and tangential excitation signals
  - Other workpiece materials such as cast iron
  - Spherical locators